PHYSICAL REVIEW B VOLUME 15, NUMBER 11 1 JUNE 1977

Ising model with antiferromagnetic next-nearest-neighbor coupling. IV. Relative magnetic scattering intensity and anomalous scattering*

John Stephenson
Physics Department, Imperial College of Science and Technology, London SW7, England†
(Received 12 January 1976)

When antiferromagnetic next-nearest-neighbor interactions are introduced into an Ising model, anomalous scattering can occur on certain lattice systems, in the sense that isotherms of the reciprocal scattering intensity versus the square of the wave number can acquire (in theory) negative initial slopes at sufficiently high temperatures. Scattering from cubic lattices has only normal Ornstein-Zernike form for small wave number. The general dependence of the scattering on wave vector across the Brillouin zone is investigated at high temperatures, where it may be expressed as (direction-dependent) truncated Fourier series. The anomalous scattering from two exactly soluble one-dimensional models is analyzed, and the possibility of actually detecting anomalous scattering from one-dimensional magnetic systems is raised.

I. INTRODUCTION

The introduction of a competing interaction into a magnetic system gives rise to certain novel and characteristic features. The spin pair correlation function in the disordered phase of a ferromagnet exhibits short-range order, and its decay with increasing spin separation is dominated by an exponential function. When a competing interaction is present the pair correlation function may become oscillatory at high temperatures above a precisely located temperature T_D, the "disorder point." This feature of the pair correlation function can occur for a variety of model systems, such as the one-dimensional system of interacting classical quadrupoles solved by Thorpe and Blume,[1] and the spin-phonon interaction model of a compressible Ising magnet of Bolton and Lee,[2] discussed by Enting.[3] The case of most interest for ferromagnetism is that of the Ising model with ferromagnetic nearest-neighbor (nn) interactions, and competing antiferromagnetic next-nearest-neighbor (nnn) interactions.[4] It is understood that the nn interaction is sufficiently strong to determine the ground state. For two- and three-dimensional lattices there will be an ordered phase below the Curie point T_C, and a disordered phase above T_C. In the presence of the antiferromagnetic nnn interaction, the short-range-order phase above T_C is divided into two regions by the disorder point T_D. The spin pair correlation function decays exponentially in magnitude throughout the disordered phase, this decay being monotonic between T_C and T_D, and oscillatory above T_D. The wavelength of oscillation may be temperature dependent (disorder point of the first kind) or independent of temperature (disorder point of the second kind). In one dimension, ordering occurs only at zero temperature for these finite-range interaction models. The disordered phase then extends over the entire temperature range $0 < T < \infty$, and may be divided into two regions by the disorder point T_D, as described above.

The question naturally arises as to whether a disorder point can be detected and measured for a lattice system. Unfortunately we cannot yet give an affirmative answer to this question. Therefore it seems reasonable that one should investigate the effects of a competing interaction on quantities which involve pair correlation functions, and which *can* be measured directly for a magnetic lattice system.

The purpose of this paper is to investigate the changes which occur in the relative magnetic scattering intensity when nnn interactions are present in the Ising model of a ferromagnet. We shall discuss in Sec. II the relative magnetic scattering intensity first from a qualitative viewpoint, and then give details of the calculation in Secs. III and IV, including results for two exactly soluble one-dimensional models in Sec. V. In the succeeding paper of this series we shall show how to estimate the disorder point on a variety of Ising lattices with nnn antiferromagnetic interactions. A preliminary report of some of the results of this investigation has been presented elsewhere.[5]

II. RELATIVE MAGNETIC SCATTERING INTENSITY

The relative magnetic scattering intensity χ in the static approximation is equal to the lattice Fourier transform of the spin pair correlation function. In general χ will depend on both the magnitude q and the direction $\hat{\mathbf{e}}$ (a unit vector) of the wave vector $\vec{\mathbf{q}} = q\hat{\mathbf{e}}$, as well as on the temperature T. Considered as a function of $\vec{\mathbf{q}}$ across the Brillouin zone, $\chi(\vec{\mathbf{q}})$ will have the periodicity of the reciprocal lattice. For sufficiently small wave

number q, χ will have approximately normal Ornstein-Zernike form (Lorentzian in q^2), with spherical symmetry. In the absence of competing interactions, the second moment of the pair correlation function will be positive, and isotherms of χ^{-1} vs q^2 will be approximately linear for small q, with positive slopes. When antiferromagnetic competing interactions are present, the possibility of anomalous scattering arises. That is, at sufficiently high temperatures the second moment of the pair correlation function may become negative and χ^{-1} vs q^2 isotherms may acquire negative slopes for small q. We shall show below that anomalous scattering can occur for one-dimensional chains when the antiferromagnetic nnn interaction lies between $\frac{1}{4}$ and $\frac{1}{2}$ the nn interaction in strength. The scattering is normal for weaker values of the nnn interaction. This result acquires some interest since it is now possible to produce effectively one-dimensional magnetically interacting systems, embedded in three-dimensional crystalline matrices, with negligible interactions in the transverse directions. In two and three dimensions we can exclude anomalous scattering on cubic lattices. There is, however, still the theoretical possibility of anomalous scattering on the diamond lattice.

The behavior of the magnetic scattering intensity $\chi(\vec{q})$ across the Brillouin zone is modified by the introduction of the nnn interaction. This can be demonstrated most easily at high temperatures, where χ is determined essentially by the lattice generating function. In any selected direction $\vec{e}$ parallel to a reciprocal-lattice vector, χ can be expanded in a truncated Fourier series to order $1/T$ in temperature. The characteristic periodicity is determined by the direction $\vec{e}$, taking into account the lattice generating functions for both nn and nnn lattices. The total magnetic scattering involves a linear combination of the lattice generating functions weighted by the appropriate interactions. As the antiferromagnetic nnn interaction strength increases, one passes smoothly from the nn lattice at one extreme to the antiferromagnetic nnn lattice at the other. It seems reasonable to suggest that the high-temperature magnetic scattering data should reveal the presence of nnn interactions, and, when fitted to appropriate truncated Fourier series, should permit a quantitative estimate of the interaction strength to be made. It is perhaps worth mentioning that both the high-temperature magnetic scattering intensity and the low-temperature spin-wave spectrum are, in theory, determined by the *same* combination of nn and nnn lattice generating functions. It might therefore be instructive to make a comparative study of these quantities.

III. MAGNETIC SCATTERING AT SMALL WAVE NUMBERS

The relative magnetic scattering intensity in the static approximation at wave vector $\vec{q} = q\vec{e}$ and temperature T is equal to the lattice Fourier transform of the spin pair correlation function $\Gamma(\vec{r})$:

$$\chi = \chi(\vec{q}, T) = \sum_{\vec{r}} e^{i\vec{q}\cdot\vec{r}}\Gamma(\vec{r}) \ . \tag{3.1}$$

For a spin-$\frac{1}{2}$ Ising lattice with "spin" $\sigma_{\vec{r}} = \pm 1$ at lattice site $\vec{r}$,

$$\Gamma(\vec{r}) = \langle \sigma_{\vec{0}}\sigma_{\vec{r}} \rangle \ . \tag{3.2}$$

For the present, we limit our discussion to cubic lattices. At sufficiently small wave number q we can expand χ for a d-dimensional cubic lattice as

$$\chi(\vec{q}, T) = \chi(\vec{0}, T) - \frac{q^2}{2d}\sum_{\vec{r}} r^2\Gamma(\vec{r}) + \cdots \ , \tag{3.3}$$

which to order q^2 is independent of the direction of $\vec{q}$. The scattering will have *normal* Ornstein-Zernike form when the second moment of the pair correlation function is positive. When antiferromagnetic interactions are present, the possibility of *anomalous* scattering arises:

$$\sum_{\vec{r}} r^2\Gamma(\vec{r}) \begin{cases} >0, & \text{normal} \\ <0, & \text{anomalous} \ . \end{cases} \tag{3.4}$$

For the Ising model at sufficiently high temperatures, we can expand the coefficient of q^2 to first order in $1/T$:

$$\chi(\vec{q}, T) = \chi(\vec{0}, T) - \frac{1}{k_B T}\,\frac{q^2}{2d}\sum_{\vec{r}} r^2 J(\vec{r}) + \cdots \ . \tag{3.5}$$

Here k_B is Boltzmann's constant and $J(\vec{r})$ is the interaction between spins separated by a vector $\vec{r}$. At high temperatures the scattering will be normal or anomalous according as the second moment of $J(\vec{r})$ is positive or negative.

Next, suppose a central lattice site is coupled with q_1 nearest neighbors $\{\vec{a}_1\}$ all at distance $a_1 = |\vec{a}_1|$ through interaction $J_1 = J(\vec{a}_1)$, and with q_2 next-nearest neighbors $\{\vec{a}_2\}$ all at distance $a_2 = |\vec{a}_2|$ through interaction $J_2 = J(\vec{a}_2)$. Then

$$\chi(\vec{q}, T) = \chi(\vec{0}, T) - (1/k_B T)(q^2/2d) \times (q_1 J_1 a_1^2 + q_2 J_2 a_2^2) + \cdots \ . \tag{3.6}$$

The sign of the final parentheses factor must now be ascertained, by combining a physical and a geometrical condition.

(i) The physical condition that the nn interaction J_1 should determine the ground state when the nnn interaction J_2 is negative and antiferromagnetic is

$$\rho \equiv q_2 J_2/q_1|J_1| > -\tfrac{1}{2} \tag{3.7}$$

for a variety of Ising lattices, including the cubic lattices.[4]

(ii) Also, for cubic Bravais lattices, the ratio of nnn to nn lattice spacings is

$$a_2/a_1 = 2 \text{ in one dimension,} \qquad a_2/a_1 \leq \sqrt{2} \text{ in two and three dimensions .} \tag{3.8}$$

Combining these two conditions, we find that the scattering always has *normal* Ornstein-Zernike form in two and three dimensions, but is anomalous at sufficiently high temperatures in one dimension when

$$-\tfrac{1}{2} < \rho < -\tfrac{1}{4} . \tag{3.9}$$

For certain other lattices, investigated below, *anomalous* scattering can occur at sufficiently high temperatures for certain directions of the wave vector $\vec{q}$ when ρ lies in an appropriate range.

For the diamond lattice with nn and nnn interactions at high temperatures when q is small,

$$\chi(\vec{q}, T) = 1 + 4K_1 + 12K_2 - \tfrac{1}{6}(qa_1)^2(4K_1 + 32K_2) , \tag{3.10}$$

where

$$K_l = J_l/k_B T, \quad l = 1, 2 . \tag{3.11}$$

The nn interaction determines the ground state when $\rho > -\frac{3}{4}$, and the scattering is anomalous when

$$-\tfrac{3}{4} < \rho < -\tfrac{3}{6} . \tag{3.12}$$

Anomalous scattering can also occur on certain two-dimensional lattices. For example, the high-temperature form of χ for the triangular lattice $t(1, 2)$ is

$$\chi(\vec{q}, T) = 1 + 6K_1 + 6K_2 - \tfrac{1}{4}(qa_1)^2(6K_1 + 18K_2) . \tag{3.13}$$

The nn interaction determines the ground state when $\rho > -\frac{1}{2}$ (see Appendix A), and the scattering is anomalous when

$$-\tfrac{1}{2} < \rho < -\tfrac{1}{3} . \tag{3.14}$$

The results of this section are summarized in Table I which contains the small-wave-number forms of χ to order q^2, and various other lattice information including the ratios of nnn to nn lattice spacings (a_2/a_1), the critical values of the interaction ratio $r = J_2/|J_1|$ above which the nn interaction determines the ground state, and the corresponding values of the parameter ρ, defined in (3.7).

IV. SCATTERING AT HIGH TEMPERATURES FOR A GENERAL WAVE VECTOR $\vec{q}$

Scattering at high temperatures for a general wave vector $\vec{q}$ in reciprocal space is described through the expansion of χ to first order in $1/T$ by

$$\chi(\vec{q}, T) = 1 + \hat{J}(\vec{q})/k_B T + \cdots , \tag{4.1}$$

where

$$\hat{J}(\vec{q}) = \sum_{\vec{r}} e^{i\vec{q}\cdot\vec{r}} J(\vec{r}) \tag{4.2}$$

is the lattice Fourier transform of the Ising interaction $J(\vec{r})$. It is convenient to introduce the dimensionless quantity

$$K(\vec{r}) = J(\vec{r})/k_B T , \tag{4.3}$$

and write

$$\chi(\vec{q}, T) = 1 + \hat{K}(\vec{q}) + \cdots , \tag{4.4}$$

where $\hat{K}(\vec{q})$ is the lattice Fourier transform of $K(\vec{r})$ defined by analogy with (4.2). When nn and nnn Ising interactions are present, $\hat{J}$ and $\hat{K}$ can be written conveniently in terms of the nn and nnn fundamental lattice generating functions

$$q_1\gamma_1(\vec{q}) = \sum_{\{\vec{a}_1\}} e^{i\vec{q}\cdot\vec{r}} , \qquad q_2\gamma_2(\vec{q}) = \sum_{\{\vec{a}_2\}} e^{i\vec{q}\cdot\vec{r}} . \tag{4.5}$$

Then we have the high-temperature form of the relative magnetic scattering intensity to order $1/T$, using the notation of (3.11):

$$\chi(\vec{q}, T) = 1 + q_1 K_1 \gamma_1(\vec{q}) + q_2 K_2 \gamma_2(\vec{q}) + \cdots . \tag{4.6}$$

The relevant lattice generating functions for cubic lattices for general wave vector $\vec{q}$ are listed in Table II. Formulas for $\hat{K}(\vec{q})$ on a variety of lattices in certain selected directions $\vec{e}$ (unit vector) of the wave vector $\vec{q} = q\vec{e}$ are presented in Table III.

The relative magnetic scattering intensity in a reciprocal-lattice direction $\vec{e}$ has the general high-temperature form to order $1/T$, of a truncated Fourier series decomposition:

$$\chi(q\vec{e}, T) = (1 + c_{01}K_1 + c_{02}K_2 + \cdots) + (c_{11}K_1 + c_{12}K_2 + \cdots)\cos f q a_1 + (c_{21}K_1 + c_{22}K_2 + \cdots)\cos 2f q a_1 + \cdots , \tag{4.7}$$

where the numerical coefficients c_{ij} and projection factors f depend on the direction $\vec{e}$ and are listed in Table III. It is perhaps worth remarking that χ can be so expanded in terms of a single

TABLE I. Lattice data and the relative magnetic scattering intensity $\chi(\vec{q}, T)$ at small wave number q to order $1/T$ in temperature.

Lattice [a]	q_1	q_2	r_c	ρ_c	a_1/a [b]	a_2/a_1	$\chi(\vec{q},T)$ at small q and high T [c]	Nature of scattering [d]
lc(1,2)	2	2	$-\frac{1}{2}$	$-\frac{1}{2}$	1	2	$1+2K_1+2K_2-\frac{1}{2}(qa_1)^2(2K_1+8K_2)$	Anomalous for $-\frac{1}{2}<\rho<-\frac{1}{4}$
lca(1,2)	2	1 [e]	−1	$-\frac{1}{2}$	1	2	$1+2K_1+K_2-\frac{1}{2}(qa_1)^2(2K_1+4K_2)$	Anomalous for $-\frac{1}{2}<\rho<-\frac{1}{4}$
sq(1,2)	4	4	$-\frac{1}{2}$	$-\frac{1}{2}$	1	$\sqrt{2}$	$1+4K_1+4K_2-\frac{1}{4}(qa_1)^2(4K_1+8K_2)$	Normal
h(1,2)	3	6	$-\frac{1}{4}$	$-\frac{1}{2}$	···	$\sqrt{3}$	$1+3K_1+6K_2-\frac{1}{4}(qa_1)^2(3K_1+18K_2)$	Anomalous for $-\frac{1}{2}<\rho<-\frac{1}{3}$
t(1,2)	6	6	$-\frac{1}{2}$	$-\frac{1}{2}$	···	$\sqrt{3}$	$1+6K_1+6K_2-\frac{1}{4}(qa_1)^2(6K_1+18K_2)$	Anomalous for $-\frac{1}{2}<\rho<-\frac{1}{3}$
sc(1,2)	6	12	$-\frac{1}{4}$	$-\frac{1}{2}$	1	$\sqrt{2}$	$1+6K_1+12K_2-\frac{1}{6}(qa_1)^2(6K_1+24K_2)$	Normal
bcc(1,2)	8	6	$-\frac{2}{3}$	$-\frac{1}{2}$	$\frac{1}{2}\sqrt{3}$	$2/\sqrt{3}$	$1+8K_1+6K_2-\frac{1}{6}(qa_1)^2(8K_1+8K_2)$	Normal
fcc(1,2)	12	6	−1	$-\frac{1}{2}$	$1/\sqrt{2}$	$\sqrt{2}$	$1+12K_1+6K_2-\frac{1}{6}(qa_1)^2(12K_1+12K_2)$	Normal
d(1,2)	4	12	$-\frac{1}{4}$	$-\frac{3}{4}$	$\frac{1}{4}\sqrt{3}$	$2(\frac{2}{3})^{1/2}$	$1+4K_1+12K_2-\frac{1}{6}(qa_1)^2(4K_1+32K_2)$	Anomalous for $-\frac{3}{4}<\rho<-\frac{3}{8}$
t as sq plus one set of nnn bonds	4	2	−1	$-\frac{1}{2}$	1	$\sqrt{2}$	$1+4K_1+2K_2-\frac{1}{4}(qa_1)^2\times\begin{cases}4K_1+4K_2\\4K_1+8K_2\\4K_1\end{cases}$	nn axis, normal nnn axis, anomalous for $-\frac{1}{2}<\rho<-\frac{1}{4}$ perpendicular to nn axis, normal
t triangular in shape	4	2	−1	$-\frac{1}{2}$	···	1	$1+4K_1+2K_2-\frac{1}{4}(qa_1)^2\times\begin{cases}5K_1+K_2\\2K_1+4K_2\\3K_1+3K_2\end{cases}$	nn axis, normal nnn axis, anomalous for $-\frac{1}{2}<\rho<-\frac{1}{4}$ perpendicular to nn axis, normal
union jack	4	2 [e]	−1	$-\frac{1}{2}$	1	$\sqrt{2}$	Replace K_2 by $\frac{1}{2}K_2$ in sq(1,2)	Normal
fcc as bcc plus sq layers	8	4	−1	$-\frac{1}{2}$	$\frac{1}{2}\sqrt{3}$	$2/\sqrt{3}$	$1+8K_1+4K_2-\frac{1}{6}(qa_1)^2(8K_1+8K_2)$	Normal along nnn axis
Same as above, fcc in shape	8	4	−1	$-\frac{1}{2}$	$1/\sqrt{2}$	1	$1+8K_1+4K_2-\frac{1}{6}(qa_1)^2(6K_1+6K_2)$	Normal along nnn axis

[a] Lattice notation is as follows: (1,2) denotes presence of first- and second-nearest-neighbor interactions; lc: linear chain with all second-nearest-neighbor interactions present, Fig. 4(a); lca: linear chain with alternate second-neighbor interactions, Fig. 4(b); sq: simple quadratic or square lattice; h: honeycomb, Fig. 4(c); t: triangular lattice, Fig. 4(d); sc: simple cubic; bcc: body-centered cubic; fcc: face-centered cubic; d: diamond; the triangular lattice t as a square lattice plus one set of nnn bonds is illustrated in Fig. 4(f); the union-jack lattice is illustrated in Fig. 4(e).

[b] a, cube side length; a_1, nn spacing; a_2, nnn spacing.

[c] For the first nine lattices, χ is independent of direction to order q^2.

[d] $\rho = q_2\gamma/q_1 = q_2J_2/q_1J_1$, with $J_1 > 0$.

[e] Effective coordination number.

TABLE II. Lattice generating functions for cubic lattices; $\vec{q}=q_x\vec{i}+q_y\vec{j}+q_z\vec{k}$, a=cube side.

Simple cubic	$q_1\gamma_1=2(\cos q_xa+\cos q_ya+\cos q_za)$
	$q_2\gamma_2=4(\cos q_xa\cos q_ya+\cos q_ya\cos q_za+\cos q_za\cos q_xa)$
Body-centered cubic	$q_1\gamma_1=8\cos\frac{1}{2}q_xa\cos\frac{1}{2}q_ya\cos\frac{1}{2}q_za$
	$q_2\gamma_2=2(\cos q_xa+\cos q_ya+\cos q_za)$
Face-centered cubic	$q_1\gamma_1=4(\cos\frac{1}{2}q_xa\cos\frac{1}{2}q_ya+\cos\frac{1}{2}q_ya\cos\frac{1}{2}q_za+\cos\frac{1}{2}q_za\cos\frac{1}{2}q_xa)$
	$q_2\gamma_2=2(\cos q_xa+\cos q_ya+\cos q_za)$

TABLE III. Formulas for $\hat{K}(\vec{q})$ in certain selected directions $\vec{e}$ of the wave vector $\vec{q}$. The lattice notation is explained in Table I, footnote (a).

Lattice	Direction	$\vec{e}$	f^2	$\hat{K}(\vec{q})$ in direction $\vec{e}$; $x=fqa_1$
lc(1,2)	Along chain, nn and nnn axis	$\vec{i}$	1	$2K_1\cos x+2K_2\cos 2x$
lca(1,2)	Along chain, nn and nnn axis	$\vec{i}$	1	$2K_1\cos x+K_2\cos 2x$
sq(1,2)	Along sq edge, nn axis	$\vec{i}$	1	$2K_1+(2K_1+4K_2)\cos x$
	Along sq diagonal, nnn axis	$(\vec{i}+\vec{j})/\sqrt{2}$	$\frac{1}{2}$	$2K_2+4K_1\cos x+2K_2\cos 2x$
	Along [21] direction	$(2\vec{i}+\vec{j})/\sqrt{5}$	$\frac{1}{5}$	$(2K_1+2K_2)\cos x+2K_1\cos 2x+2K_2\cos 3x$
h(1,2)	Along nn direction	$\vec{i}$	$\frac{1}{4}$	$2K_2+2K_1\cos x+K_1\cos 2x+4K_2\cos 3x$
	Along nnn direction	$\vec{j}$	$\frac{3}{4}$	$K_1+(2K_1+4K_2)\cos x+2K_2\cos 2x$
t(1,2)	Along nn axis	$\vec{i}$	$\frac{1}{4}$	$2K_2+4K_1\cos x+2K_1\cos 2x+4K_2\cos 3x$
	Along nnn axis	$\vec{j}$	$\frac{3}{4}$	$2K_1+(4K_1+4K_2)\cos x+2K_2\cos 2x$
sc(1,2)	Along cube edge, nn axis	$\vec{i}$	1	$4K_1+4K_2+(2K_1+8K_2)\cos x$
	Along face diagonal, nnn axis	$(\vec{i}+\vec{j})/\sqrt{2}$	$\frac{1}{2}$	$2K_1+2K_2+(4K_1+8K_2)\cos x+2K_2\cos 2x$
	Along body diagonal, third-nn axis	$(\vec{i}+\vec{j}+\vec{k})/\sqrt{3}$	$\frac{1}{3}$	$6K_2+6K_1\cos x+6K_2\cos 2x$
	Along [210] direction	$(2\vec{i}+\vec{j})/\sqrt{5}$	$\frac{1}{5}$	$2K_1+(2K_1+6K_2)\cos x+(2K_1+4K_2)\cos 2x+2K_2\cos 3x$
bcc(1,2)	Along cube edge, nnn axis	$\vec{i}$	$\frac{1}{3}$	$4K_2+8K_1\cos x+2K_2\cos 2x$
	Along face diagonal, third-nn axis	$(\vec{i}+\vec{j})/\sqrt{2}$	$\frac{2}{3}$	$4K_1+2K_2+(4K_1+4K_2)\cos x$
	Along body diagonal, nn axis	$(\vec{i}+\vec{j}+\vec{k})/\sqrt{3}$	$\frac{1}{9}$	$6K_1\cos x+6K_2\cos 2x+2K_1\cos 3x$
fcc(1,2)	Along cube edge, nnn axis	$\vec{i}$	$\frac{1}{2}$	$4K_1+4K_2+8K_1\cos x+2K_2\cos 2x$
	Along face diagonal, nn axis	$(\vec{i}+\vec{j})/\sqrt{2}$	$\frac{1}{4}$	$2K_1+2K_2+8K_1\cos x+(2K_1+4K_2)\cos 2x$
	Along body diagonal	$(\vec{i}+\vec{j}+\vec{k})/\sqrt{3}$	$\frac{2}{3}$	$6K_1+(6K_1+6K_2)\cos x$
d(1,2)	Along cube edge, nnn direction	$\vec{i}$	$\frac{2}{3}$	$2K_1+2K_2+(2K_1+8K_2)\cos x+2K_2\cos 2x$
t as sq	Along sq edge, nn axis	$\vec{i}$	1	$2K_1+(2K_1+2K_2)\cos x$
plus one set	Along sq diagonal, nnn axis	$(\vec{i}+\vec{j})/\sqrt{2}$	$\frac{1}{2}$	$4K_1\cos x+2K_2\cos 2x$
of nnn bonds	Along sq diagonal, perpendicular to nnn axis	$(-\vec{i}+\vec{j})/\sqrt{2}$	$\frac{1}{2}$	$2K_2+4K_1\cos x$
t	Along nn axis	$\vec{i}$	$\frac{1}{4}$	$(2K_1+2K_2)\cos x+2K_1\cos 2x$
triangular	Along nnn axis	$\frac{1}{2}(\vec{i}+\sqrt{3}\,\vec{j})$	$\frac{1}{4}$	$4K_1\cos x+2K_2\cos 2x$
in shape	perpendicular to nn axis	$\vec{j}$	$\frac{3}{4}$	$2K_1+(2K_1+2K_2)\cos x$
union-jack	Replace J_2 by $\frac{1}{2}J_2$ in formulas for sq(1,2)		...	...
fcc as bcc plus sq layers	nnn direction, along edge of an sq layer	$\vec{i}$	$\frac{1}{3}$	$2K_2+8K_1\cos x+2K_2\cos 2x$
same as above, but fcc in cubic shape	same as above	$\vec{i}$	$\frac{1}{4}$	$2K_2+8K_1\cos x+2K_2\cos 2x$

variable

$$x = fqa_1 \tag{4.8}$$

if, and only if, the relevant direction $\vec{e}$ is parallel to a reciprocal-lattice vector. A proof of this is presented in Appendix B.
At zero wave number

$$\chi(\vec{0}, T) = 1 + q_1 K_1 + q_2 K_2 + \cdots , \tag{4.9}$$

so the coefficients c_{ij} obey the trivial sum rules

$$\begin{aligned} c_{01} + c_{11} + c_{21} + \cdots &= q_1 , \\ c_{02} + c_{12} + c_{22} + \cdots &= q_2 , \end{aligned} \tag{4.10}$$

and equally trivially, the small wave-number behavior of χ has the form

$$\chi(\vec{q}, T) = \chi(\vec{0}, T) - (q^2 a_1^2/2d)(b_1 K_1 + b_2 K_2 + \cdots) , \tag{4.11}$$

where the numerical coefficients $b_1, b_2, \ldots$ are given by linear combinations of the c_{ij}.

The changes in the form of the scattering intensity brought about by the nnn interaction are direction dependent on a given lattice, and emerge clearly from the truncated Fourier series expansion for $\chi(\vec{q}, T)$ at *high* temperatures. It is then convenient to work in terms of the temperature-independent quantity

$$k_B T[\chi(\vec{q}, T) - 1] = \hat{J}(\vec{q}) \tag{4.12}$$

in the suitably normalized form $\hat{J}(\vec{q})/J$, where

$$J = [(q_1 J_1)^2 + (q_2 J_2)^2]^{1/2} , \tag{4.13}$$

to allow for extreme cases. Graphs of $\hat{J}(\vec{q})/J$ are presented in Figs. 1–3 for the three cubic lattices in the [100], [110], and [111] directions. The effects of the antiferromagnetic nnn interaction can be observed directly.

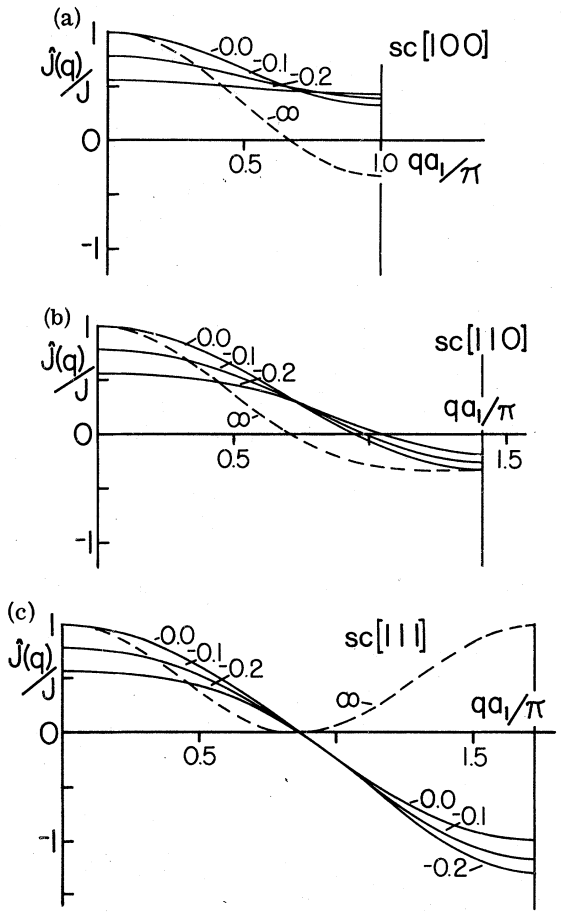

FIG. 1. Lattice Fourier transforms $\hat{J}(\vec{q})/J$ for the simple cubic lattice in the [100], [110], and [111] directions. See text, Sec. IV (4.12) and (4.13). The graphs are labeled with the corresponding values of $J_2/|J_1|$.

V. ONE-DIMENSIONAL MODELS

In this section we discuss two linear chain models with next-nearest-neighbor interactions. These models have been solved exactly and exhibit disorder points.[6] Explicit expressions for the pair correlation functions are available, and it is straightforward to calculate closed-form exact expressions for the relative magnetic scattering intensity. These can be used to test both our approximate calculations of Secs. III and IV, and our subsequent treatment of disorder points in the following paper.

A. Linear chain with both nnn interactions lc(1,2)

For this model [see Fig. 4(a)] the pair correlation between spins separated by a vector $\vec{r}$ along the chain, with $|\vec{r}| = na_1$, where a_1 is the nn lattice spacing, is

$$\Gamma(\vec{r}) = \tfrac{1}{2}[(1+\alpha)(\mu_+/\lambda_+)^n + (1-\alpha)(\mu_-/\lambda_+)^n] , \tag{5.1}$$

with

$$\alpha = [(a^2 - b^2)/\Delta\Delta'] , \tag{5.2}$$

where in terms of K_1 and K_2,

$$\begin{aligned} \Delta &= 2e^{K_2}[(\sinh K_1)^2 + e^{-4K_2}]^{1/2} , \\ \Delta' &= 2e^{K_2}[(\cosh K_1)^2 - e^{-4K_2}]^{1/2} , \\ \lambda_\pm &= e^{K_2}\{\cosh K_1 \pm [(\sinh K_1)^2 + e^{-4K_2}]^{1/2}\} , \\ \mu_\pm &= e^{K_2}\{\sinh K_1 \pm [(\cosh K_1)^2 - e^{-4K_2}]^{1/2}\} , \\ a^2 - b^2 &= 2e^{2K_2}\sinh 2K_1 . \end{aligned} \tag{5.3}$$

The form of the pair correlation is determined primarily by whether $\mu_\pm$ are real or complex. λ_+ is real and positive, and quite generally $|\mu_\pm/\lambda_+| < 1$, so there is only a disordered phase. The change from real to complex $\mu_\pm$ occurs when Δ'

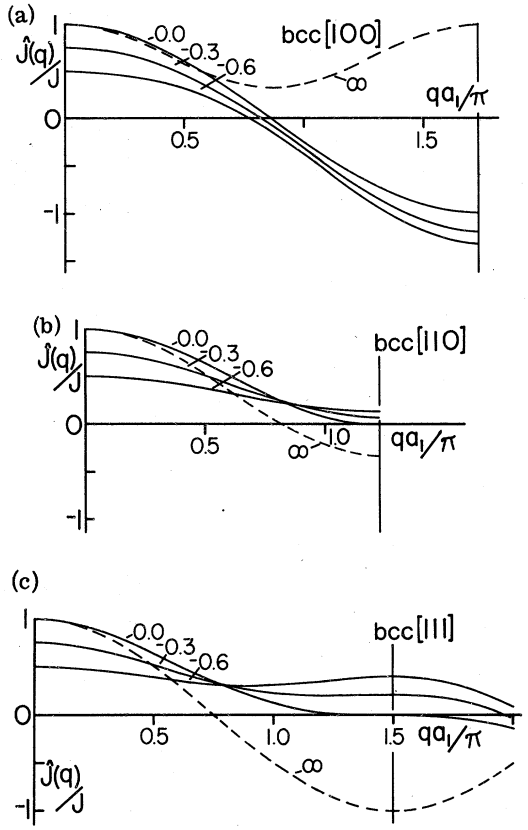

FIG. 2. Lattice Fourier transforms $\hat{J}(\vec{q})/J$ for the body-centered-cubic lattice in the [100], [110], and [111] directions. See text, Sec. IV (4.12) and (4.13). The graphs are labeled with the corresponding values of $J_2/|J_1|$.

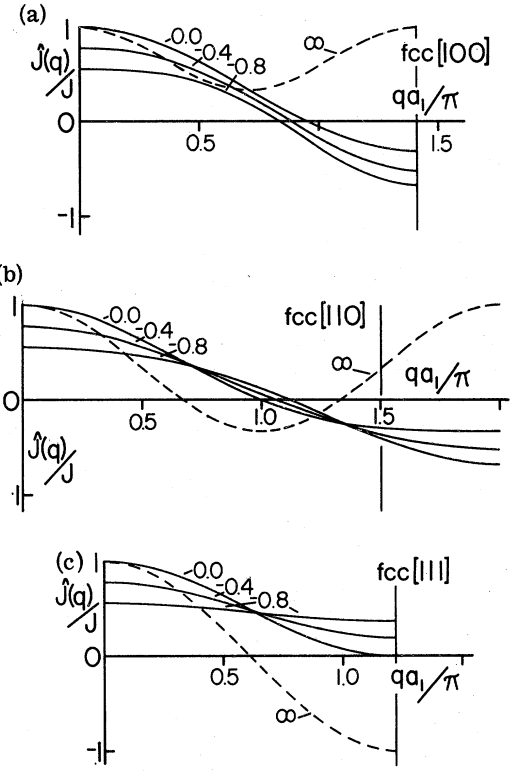

FIG. 3. Lattice Fourier transforms $\hat{J}(\vec{q})/J$ for the face-centered-cubic lattice in the [100], [110], and [111] directions. See text, Sec. IV (4.12) and (4.13). The graphs are labeled with the corresponding values of $J_2/|J_1|$.

$=0$, or

$$\cosh K_1 = e^{-2K_2} ,$$

or (5.4)

$$\tanh K_2 + (\tanh \tfrac{1}{2}K_1)^2 = 0 ,$$

which has a solution when $-\frac{1}{2}|J_1| < J_2 < 0$ at some finite temperature T_D, the disorder point. Δ' is real below T_D and pure imaginary above, so the decay of pair correlations is monotonic exponential below T_D and oscillatory exponential above T_D, with temperature-dependent wavelength. Above T_D, $\mu_\pm$ are complex, and we can set $\mu_\pm = \mu e^{i\theta}$, where μ and θ are real and positive. Then

$$\Gamma(\vec{r}) = \left(\frac{\mu}{\lambda_+}\right)^n \left[\left(\frac{a^2-b^2}{\Delta|\Delta'|}\right)\sin n\theta + \cos n\theta\right] \tag{5.5}$$

displaying the oscillatory decay of the pair correlation, with wavelength $2\pi a_1/\theta$.

Explicit calculation of χ is straightforward, with the result

$$\chi(\vec{q}, T) = \frac{\frac{1}{2}(1+\alpha)(1-x^2)}{1-2x\cos q + x^2} + \frac{\frac{1}{2}(1-\alpha)(1-y^2)}{1-2y\cos q + y^2} , \tag{5.6}$$

where we have used the abbreviations

$$x = \mu_+/\lambda_+ , \quad \text{and} \quad y = \mu_-/\lambda_+ . \tag{5.7}$$

Since x, y, and α can take complex values, it is useful to rearrange the above expression in terms of the real quantities:

$$\begin{aligned} x + y &= (2e^{K_2}\sinh K_1)/\lambda_+ \sim K_1 , \\ xy &= -(2\sinh 2K_2)/\lambda_+^2 \sim -K_2 , \\ \beta &= \alpha\Delta'/\lambda_+ = (a^2-b^2)/\Delta\lambda_+ \sim K_1 . \end{aligned} \tag{5.8}$$

We have also written down the high-temperature behavior of these quantities, since it is needed later. It is evident that χ can be written in the form $\chi = N/D$ with numerator and denominator normalized to unity at infinite temperature, and given by

$$N=(1-x^2y^2)+\beta(x+y)$$
$$-\cos q[(x+y)(1-xy)-\beta(1+xy)]\ , \qquad (5.9)$$
$$D=(1-2x\cos q+x^2)(1-2y\cos q+y^2)\ .$$

Next, we illustrate graphically the anomalous scattering which occurs when $-\frac{1}{2}<\rho<-\frac{1}{4}$, with $\rho=J_2/|J_1|$. Isotherms of $1/\chi$ vs $(q/\pi)^2$ are plotted in Fig. 5 for the typical case $J_2/|J_1|=-0.3$. At sufficiently high temperatures these graphs have negative initial slopes. These properties characterize anomalous scattering. Further, in Fig. 6, we have plotted the coefficient of q^2 in χ^{-1}, which determines the initial slopes of the χ^{-1} vs $(q/\pi)^2$ graphs, against temperature in units of $|J_1|/k_B$, for various fixed values of the interaction ratio $\rho=J_2/|J_1|$. These graphs illustrate how the initial slopes change sign, and the scattering becomes anomalous, at sufficiently high temperatures when $-\frac{1}{2}<\rho<-\frac{1}{4}$, but remains normal when $-\frac{1}{4}<\rho<0$.

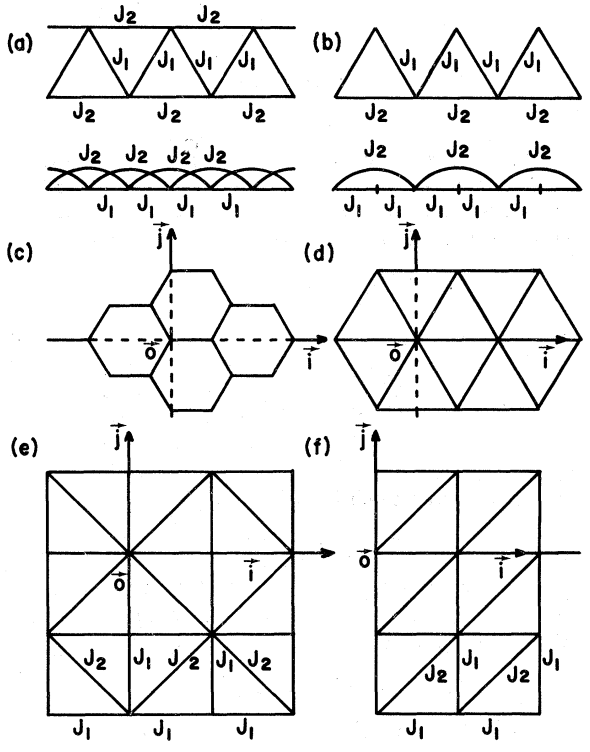

FIG. 4. Diagrams of some of the one- and two-dimensional lattices discussed in the text and tables. (a) Linear chain with nn and nnn interactions, lc(1,2); (b) linear chain with alternate nnn interactions, lca(1,2); (c) honeycomb; (d) triangular; (e) union-jack; (f) triangular lattice as a simple quadratic (square, sq) lattice plus single nnn diagonal bonds.

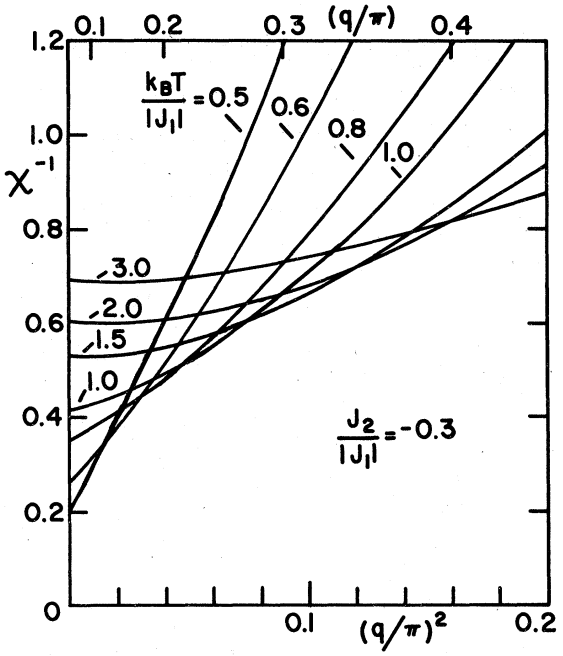

FIG. 5. Graphs of the reciprocal relative magnetic scattering intensity χ^{-1} vs the square of the wave number $(q/\pi)^2$ for the linear chain lc(1,2) with interaction ratio $J_2/|J_1|=-0.3$ at various temperatures in the scaled form $k_BT/|J_1|$. The top horizontal scale is q/π.

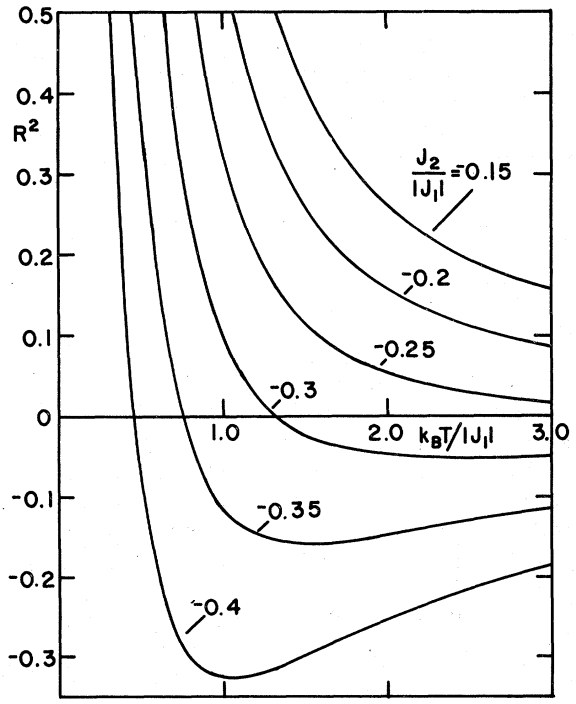

FIG. 6. Graphs of R^2, the coefficient of q^2 in the reciprocal scattering intensity χ^{-1}, plotted vs temperature for the linear chain lc(1,2) for various values of the interaction ratio $J_2/|J_1|$.

B. Linear chain with alternate nnn interactions lca(1,2)

This model is illustrated in Fig. 4(b). We list the relevant formulas for pair correlations and the relative magnetic scattering intensity. Let s_i denote spins linked by the nnn interaction J_2, and σ_i denote intermediate spins linked only to adjacent nearest-neighbor s spins by the nn interaction J_1. Then for spin separation $na_1=(j-i)a_1$ between lattice sites i and j, with $j>i$, we have:

$$\begin{aligned}&\langle s_i s_j\rangle = x^{n/2}, \quad n \text{ even}\\ &\langle s_i \sigma_j\rangle = x^{(n-1)/2} y, \quad n \text{ odd}\\ &\langle \sigma_i \sigma_j\rangle = x^{(n/2)-1} y^2, \quad n \text{ even}\end{aligned} \tag{5.10}$$

where in terms of K_1 and K_2,

$$\begin{aligned}x &= \frac{\cosh 2K_1 - e^{-2K_2}}{\cosh 2K_1 + e^{-2K_2}} \sim K_2 ,\\ y &= \frac{\sinh 2K_1}{\cosh 2K_1 + e^{-2K_2}} \sim K_1 ,\end{aligned} \tag{5.11}$$

and on the extreme right-hand side we have written down the high-temperature behavior of these quantities. It is straightforward to calculate χ, which has the form N/D with

$$\begin{aligned}N &= (1-xy^2) + 2y(1-x)\cos q + (y^2-x)\cos 2q ,\\ D &= 1 - 2x\cos 2q + x^2 .\end{aligned} \tag{5.12}$$

It is easy to see from these expressions for the pair correlations that a change in their form takes place at a temperature T_D, the disorder point, located by

$$\cosh 2K_1 = e^{-2K_2} \tag{5.13}$$

or

$$(\tanh K_1)^2 + \tanh K_2 = 0 ,$$

which has a solution when $-|J_1|<J_2<0$. There is only one phase, which is disordered, and the decay of pair correlations with increasing spin separation is exponential at all temperatures, except zero. Below T_D the decay is monotonic, whereas above T_D it is oscillatory. The wavelength of oscillation is independent of temperature.

The scattering is anomalous at sufficiently high temperatures when $-\frac{1}{2}<\rho<-\frac{1}{4}$, but remains normal when $-\frac{1}{4}<\rho<0$. This is illustrated by graphs of the coefficient of q^2 in χ^{-1} versus temperature in units of $|J_1|/k_B$ in Fig. 7. We do not present graphs of χ itself, since the relative scattering intensity has the same qualitative form for both the linear chains considered here.

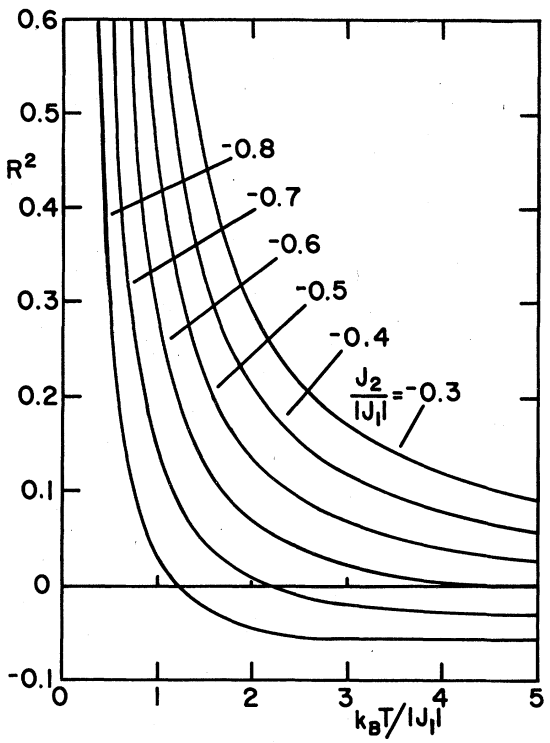

FIG. 7. Graphs of R^2, the coefficient of q^2 in the reciprocal scattering intensity χ^{-1}, plotted vs temperature for the linear chain with alternate nnn interactions lca(1,2) for various values of the interaction ratio $J_2/|J_1|$.

VI. SUMMARY

In this paper we have considered the modifications which may occur to the relative magnetic scattering intensity χ when competing antiferromagnetic next-nearest-neighbor interactions are introduced into the Ising model. We have shown that anomalous scattering can occur on certain lattice systems, including two soluble one-dimensional models, in the sense that isotherms of the reciprocal scattering intensity χ^{-1} versus the square of the wave number q^2 can acquire negative initial slope at sufficiently high temperatures, provided the relative strength of the nearest- and next-nearest-neighbor interactions lies in an appropriate range. The scattering from cubic lattices has only normal Ornstein-Zernike form for small wave number. The general dependence of χ on wave vector $\tilde{q}$ across the Brillouin zone has been investigated at high temperatures, where it depends on the lattice Fourier transform of the basic nn and nnn generating functions. The truncated Fourier series form of χ has been discussed in detail.

APPENDIX A: GROUND STATE OF THE TRIANGULAR LATTICE t(1,2)

The aim is to find the critical ratio ρ_c for the triangular lattice with antiferromagnetic nnn interactions. This particular lattice is tricky to handle

because the three nnn sublattices are themselves triangular, and antiferromagnetism is not compatible with a triangular net. One must calculate the ground-state energy first when the nn interaction is dominant and all spins are aligned, with $J_1>0>J_2$:

$$U_1=-N(3J_1+3J_2)\ , \tag{A1}$$

where N is the number of lattice sites. Next we must construct an arrangement of spins in which each of the three nnn triangular sublattices is separately in a possible antiferromagnetic ground state. In each triangle formed from nnn bonds with antiferromagnetic interaction J_2, there must be two antiparallel spin pairs and one parallel spin pair. This may be achieved as illustrated in Fig. 8. The energy of this arrangement of spins is

$$U_2=N(J_2-J_1)\ . \tag{A2}$$

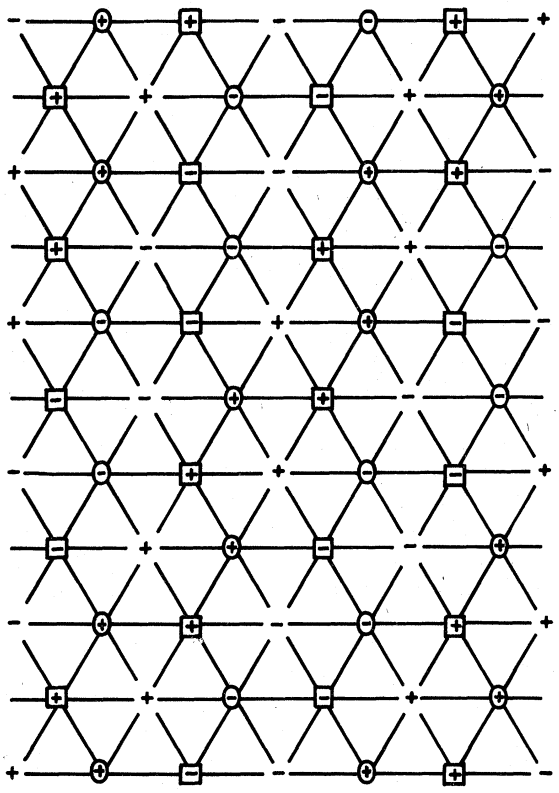

FIG. 8. Diagram of a spin arrangement for the ground state of the triangular lattice t(1,2), with $J_2<0<J_1$, when the nnn interaction J_2 is much stronger than the nn interaction J_1. Spins on the three triangular nnn sublattices are shown either surrounded by a circle or a square, or unmarked. Each triangular nnn sublattice is in a ground-state configuration. The actual overall arrangement of spins consists of two lines of "+" spins followed by two lines of "−" spins in a regular periodic (diagonal) array.

Equating U_1 and U_2 we find the critical ratio

$$\rho_c\equiv q_2J_2/q_1|J_1|=-\tfrac{1}{2}\ .$$

The result extends the table of critical ratios ρ_c given by Stephenson and Betts.[4]

APPENDIX B: FOURIER SERIES EXPANSION FOR χ

Theorem: $\chi(\vec{q}, T)$ has a Fourier series expansion in a *single* variable if and only if the direction $\vec{e}$ (unit vector) of the wave vector $\vec{q}=q\vec{e}$ is parallel to a reciprocal-lattice vector.

The proof is for a general Bravais lattice with basis vectors $\vec{b}_1, \vec{b}_2, \vec{b}_3$ and reciprocal-lattice basis vectors $\vec{b}^1, \vec{b}^2, \vec{b}^3$, satisfying the relation $\vec{b}_i\cdot\vec{b}^j=\delta_{ij}$.

(a) *If*. Suppose the unit vector $\vec{e}$ is parallel to a reciprocal-lattice vector. Then $\vec{e}$ has the form

$$\vec{e}=(a_1/N)(e_1\vec{b}^1+e_2\vec{b}^2+e_3\vec{b}^3)\ , \tag{B1}$$

with the "normalizing" factor N given by

$$N^2=a_1^2\sum_{i,j=1}^{3}e_ie_j(\vec{b}^i\cdot\vec{b}^j)\ , \tag{B2}$$

for *integer* values of e_1, e_2, e_3. Then the product $\vec{q}\cdot\vec{r}$ involved in the definition of $\chi(\vec{q}, T)$ has the form

$$\vec{q}\cdot\vec{r}=(qa_1/N)(n_1e_1+n_2e_2+n_3e_3)\ , \tag{B3}$$

in which we have set $\vec{q}=q\vec{e}$ and $\vec{r}$ is a general lattice vector,

$$\vec{r}=n_1\vec{b}_1+n_2\vec{b}_2+n_3\vec{b}_3\ , \tag{B4}$$

with n_1, n_2, n_3 integers. The right-hand side of (B3) has the form of an integer times fqa_1, where $f=1/N$. So χ has a Fourier series expansion in a single variable.

(b) *Only if*. Conversely, suppose χ has a Fourier series expansion in terms of a single variable $x=fqa_1$, say, for a direction $\vec{e}$ of the wave vector $\vec{q}=q\vec{e}$. We can quite generally write $\vec{e}$ in the form (B1), except that the e_i and N are not yet specified separately. It is required to show, for an appropriate choice of N, that the e_i are integers, in which case $\vec{e}$ will be parallel to a reciprocal-lattice vector. Now by supposition, χ has a Fourier series expansion in a single variable, so

$$\vec{q}\cdot\vec{r}=mfqa_1\ , \tag{B5}$$

where m is an integer. Calculate $\vec{q}\cdot\vec{r}$ as in (B3) for *any* lattice vector $\vec{r}$:

$$\vec{q}\cdot\vec{r}=(qa_1/N)(n_1e_1+n_2e_2+n_3e_3)\ . \tag{B6}$$

With the appropriate choice of N, viz., $N=1/f$, we find that the combination $n_1e_1+n_2e_2+n_3e_3$ is an integer, for all integers n_1, n_2, n_3. Therefore e_1, e_2, e_3 must be integers, and $\vec{e}$ will be parallel to a reciprocal-lattice vector, as required.

*Work supported in part by the National Research Council of Canada, Grant No. A6595, and in part by the Science Research Council (UK).

†On leave from Physics Department, University of Alberta, Edmonton, Alberta, Canada.

[1]M. F. Thorpe and M. Blume, Phys. Rev. B 5, 1961 (1972).

[2]H. C. Bolton and B. S. Lee, J. Phys. C 3, 1433 (1970); B. S. Lee and H. C. Bolton, *ibid.* 4, 1178 (1971).

[3]I. G. Enting, J. Phys. A 6, 170 (1973); J. Phys. C 6, 3457 (1973).

[4]J. Stephenson, J. Phys. Rev. B 1, 4405 (1970); J. Stephenson, and D. D. Betts, *ibid.* 2, 2702 (1970); J. Stephenson, J. Appl. Phys. 42, 1278 (1971).

[5]J. Stephenson, AIP Conf. Proc. 5, 357 (1971).

[6]J. Stephenson, Can. J. Phys. 48, 1724 (1970).